



Symmetrical mesogenic 2,5-bis(6-naphthalen-2-yl)-1,3,4-thiadiazoles

Hsiu-Ming Kuo^a, Sih-Yeh Li^a, Hwo-Shuenn Sheu^b, Chung K. Lai^{a,*}

^a Department of Chemistry and Center for Nano Science Technology, National Central University, Chung-Li 32001, Taiwan, ROC

^b National Synchrotron Radiation Research Center, Hsinchu 30077, Taiwan, ROC

ARTICLE INFO

Article history:

Received 28 April 2012

Received in revised form 12 June 2012

Accepted 21 June 2012

Available online 28 June 2012

ABSTRACT

Two series of new symmetrical 1,3,4-oxadiazoles **1a-n** and 1,3,4-thiadiazoles **1b-n** were prepared and their mesomorphic properties investigated by optical microscopy, differential scanning calorimetry, and powder X-ray diffractometry. Compounds **1b-n** are kinetically more stable than compounds **1a-n**. Compounds **1a-n** exhibited monotropic nematic or smectic C phases, whereas, compounds **1b-n** exhibited enantiotropic nematic or smectic A/smectic C phases. Compounds **1b-n** have higher clearing temperatures and the larger temperature ranges of mesophases, which might be attributed to the better linearity and/or larger dipole, resulted from a more polarized sulfur atom than oxygen atom incorporated. The fluorescent properties of these two series of 1,3,4-thiadiazole/oxadiazole-based derivatives were also examined. The λ_{\max} peaks of the photoluminescence spectra for compounds **1a-6** and **1b-6** measured in THF occurred at ca. 385 nm and 423 nm, respectively. Both series were blue emitters.

© 2012 Elsevier Ltd. All rights reserved.

1. Introduction

1,3,4-Oxadiazole (OXD), considered as one of the few important compounds among five-membered heterocycles, has been studied in the field of materials chemistry and biochemistry. Parts of such extensive studies originated from their excellent thermal, chemical stabilities and high photoluminescence quantum yields. The importance of 1,3,4-oxadiazoles compounds is also attributed to the simultaneous presence of a bent-shaped structure and of an electric dipole, which are often applied as a framework constructed for materials¹ with achiral molecules; useful materials with ferroelectric states might be obtained. The heterocyclic 1,3,4-oxadiazole moiety was often considered as an electron-deficient and good electron acceptor. Incorporation of appropriate electron-withdrawing and electron-donating groups on either lateral side might generate many potential materials valuable in organic light-emitting diodes (OLEDs). Numerous known 1,3,4-oxadiazoles with a variety of novel structures were studied as electron transporting materials in OLEDs. Some of them were also used as organic electron conductors.

These molecules have also been investigated in the liquid crystal field since the first mesogenic asymmetric 1,3,4-oxadiazole reported² by Dimitrowa et al. Until now, many examples of mesogenic 1,3,4-oxadiazoles with either symmetrical or asymmetrical structures were prepared and studied. A few of them were structurally derived from bis-(1,3,4-oxadiazoles).³ Typical nematic or layer

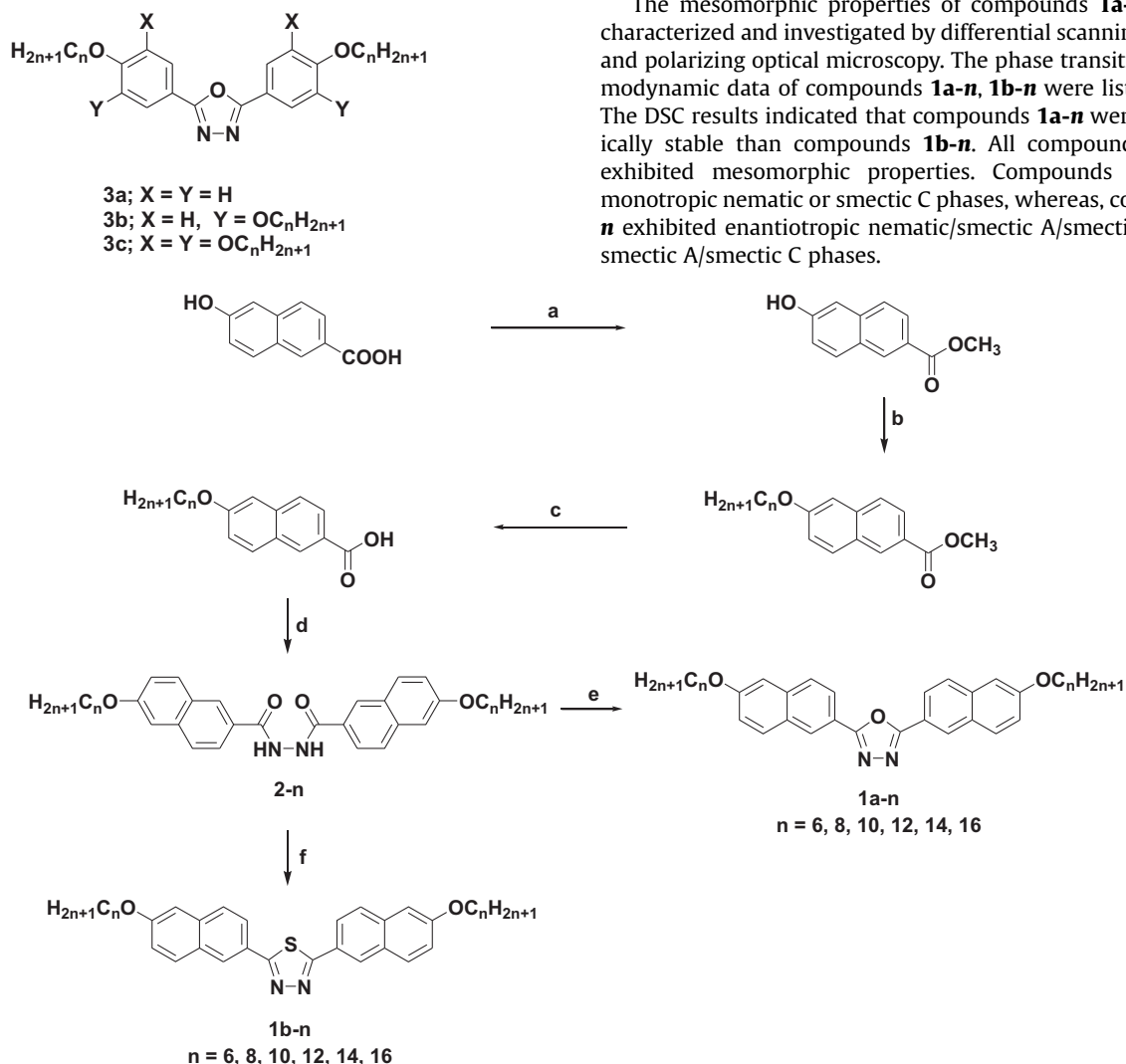
smectic phases were obtained by these linear-shaped or bent-shaped molecules. In contrast, lesser examples exhibiting columnar phases⁴ were also reported. More interestingly, the occurrence of biaxial nematic (N_b) mesophases⁵ by some 1,3,4-oxadiazole derivatives were observed, which were excellent candidates studied for liquid-crystal electro-optical display technology. Surprisingly, 2,5-bis(alkoxyphenyl)-1,3,4-oxadiazoles^{7a,b} **3a** were not liquid crystalline. 2,5-Diaryl-1,3,4-oxadiazole was considered as a non-linear structure, which was attributed to the effect of the shape formed by a larger exocyclic bond angle⁶ ($\epsilon \sim 135^\circ$). A lowering of melting or/and clearing point might be observed, and such a lowering of both melting and/or clearing temperature was demonstrated on the 2,5-bis(alkoxyphenyl)-1,3,4-oxadiazoles, **3a**^{7a,b}–**c**^{7c} and their metallomesogens^{7d} previously reported by this group. All derivatives **3a–b** were not mesogenic, whereas, other derivatives **3c** were in fact mesogenic, exhibiting room temperature columnar hexagonal phases. The lack of mesomorphism by **3a** was attributed to non-linearity⁸ caused by an exocyclic bond in the 2- and 5-positions of the oxadiazoles unit. However, the mesomorphism could be improved by incorporation of a more polar group on either side of lateral groups; for example, 2-(4-chlorophenyl)-5-(4-alkoxyphenyl)-1,3,4-oxadiazoles⁹ or other similar asymmetric structures¹⁰ exhibited nematic or smectic A phases over a wide range of temperatures. Interestingly, some derivatives of 2,5-diaryl-1,3,4-oxadiazole¹¹ without flexible chains showed enantiotropic nematic mesophases with high melting temperatures.

Their homolog 1,3,4-thiadiazoles^{6b,12} showed an apparently different mesomorphic behavior. The replacement of oxygen atom by sulfur atom often led to an improvement of liquid crystalline

* Corresponding author. Tel.: +886 (0)3 4259207; fax: +886 (0)3 4277972; e-mail address: cklai@cc.ncu.edu.tw (C.K. Lai).

behavior. The larger sulfur atom incorporated in heterocyclic rings was more easily polarized; therefore, they were better induced in forming the mesophases. Also, the longer C–S bond distance and a smaller C–S–C angle^{1c,9} of 1,3,4-thiadiazole unit often favor the formation of rod-like molecular conformations. Better linear conformations facilitated more efficient packing of molecules in the mesophases, compared to the relatively more bent-shaped 1,3,4-oxadiazoles.

In this work, we report the preparation and mesomorphic studies of two new series of symmetrical 1,3,4-oxadiazoles **1a-n** and 1,3,4-thiadiazoles **1b-n**. Two substituted 4-naphthyl lateral groups were incorporated to enhance the polarization and/or dipole needed to induce the mesophases. Also, π - π interactions often exist by neighboring two fused naphthyl rings might also better induce the formation of mesophases. Indeed, an extra smectic C phase appeared at lower temperature in **1a-n** and **1b-n** was obtained, which was not observed in other asymmetric mesogenic diphenyl-1,3,4-oxadiazole. Compounds **1a-n** indeed exhibited monotropic nematic or smectic C phases, whereas, compounds **1b-n** exhibited enantiotropic nematic or smectic A/smectic C phases. Compounds **1b-n** have higher clearing temperatures and the larger temperature ranges of mesophases than those of compounds **1a-n**, which might be attributed to a better linear conformation and larger dipole¹³ caused by the more polarized sulfur atom. Both series of compounds **1a-n**, **1b-n** were blue emitters.



Scheme 1. Reactions and reagents: (a) H₂SO₄, refluxed in CH₃OH, 2 h, 80%; (b) RBr (1.1 equiv), K₂CO₃ (1.5 equiv), KI, refluxed in acetone, 24 h, 90%; (c) KOH, refluxing in C₂H₅OH, 24 h, 93%; (d) stirred in SOCl₂, 4 h, 95%; then N₂H₄–H₂O (1.5 equiv), THF, 24 h, 80%; (e) stirred in POCl₃, 8 h, 72%; (f) P₂S₅, refluxed in pyridine, 24 h, 70%.

2. Results and discussion

2.1. Synthesis and characterization

The synthetic procedures for the compounds **1a-n**, **1b-n** are summarized in Scheme 1.

The 6-(alkoxy)-*N'*-(6-(alkoxy)-2-naphthoyl)-2-naphthohydrazides **2-n** were prepared from 6-(alkoxy)-2-naphthoic acid chlorides with an excess of hydrazine in dried THF at room temperature. The final 2,5-bis(6-(alkoxy)naphthalen-2-yl)-1,3,4-oxadiazoles **1a-n** were obtained by condensation reactions between 6-(alkoxy)-*N'*-(6-(alkoxy)-2-naphthoyl)-2-naphthohydrazides and phosphoryl chloride (POCl₃) as refluxing solvent. Replacement of POCl₃ by phosphorous trichloride (PCl₃) gave the same products with slightly lower yields. The compounds **1a-n**, **1b-n** were isolated as pale yellow to green crystals depending on the carbon chain length and the yields were in the range 63–74%. Most derivatives **1a-n**, **1b-n** were characterized by ¹H and ¹³C NMR spectroscopy, and elemental analysis. However, for some derivatives with poor solubility in organic solvents to perform NMR spectroscopy, mass spectroscopic data and elemental analysis were obtained. The ¹H NMR spectroscopy of compounds **2-n** showed one characteristic peak at ca. $\delta \sim 10.60$ ppm assigned to amide –NH.

2.2. Mesomorphic properties of compound 1a-n, 1b-n

The mesomorphic properties of compounds **1a-n**, **1b-n** were characterized and investigated by differential scanning calorimetry and polarizing optical microscopy. The phase transitions and thermodynamic data of compounds **1a-n**, **1b-n** were listed in Table 1. The DSC results indicated that compounds **1a-n** were more kinetically stable than compounds **1b-n**. All compounds **1a-n**, **1b-n** exhibited mesomorphic properties. Compounds **1a-n** formed monotropic nematic or smectic C phases, whereas, compounds **1b-n** exhibited enantiotropic nematic/smectic A/smectic C phases or smectic A/smectic C phases.

Table 1
Phase transitions and enthalpies^a of compounds **1a-n**, **1b-n**

1a-6	Cr ₁	91.2 (3.07)	Cr ₂	168.8 (39.8)	I
		81.8 (3.07)		153.9 (39.3)	
1a-8	Cr ₁	126.4 (3.65)	Cr ₂	163.8 (40.3)	I
		104.4 (3.67)		145.4 (36.3)	
1a-10	Cr ₁	119.5 (11.0)	Cr ₂	158.0 (44.8)	I
		95.6 (7.23)		147.7 (41.0)	
1a-12	Cr ₁	119.7 (10.4)	Cr ₂	155.1 (39.0)	I
		87.1 (8.06)		144.3 (33.1)	
1a-14	Cr ₁	135.1 (42.0)	Cr ₂	148.1 (33.4)	I
		119.9 (10.9)		139.8 (28.2)	
1a-16	Cr ₁	135.2 (72.2)	Cr ₂	143.2 (35.7)	I
		110.4 (65.3)		135.8 (27.0)	
1b-6	Cr	140.4 (23.7)	SmC	228.0 ^b	SmA
		110.7 (19.9)		213.9 (0.59)	
1b-8	Cr	125.9 (25.7)	SmC	197.0 ^b	SmA
		105.0 (24.0)		240.0 ^b	
1b-10	Cr	124.9 (30.5)	SmC	236.0 ^b	SmA
		106.2 (29.4)		243.0 ^b	
1b-12	Cr	239.0 ^b	SmC	237.2 (1.51)	SmA
		127.6 (37.8)		244.3 (4.69)	
1b-14	Cr	240.0 ^b	SmC	240.4 (3.96)	SmA
		115.0 (38.0)		237.0 ^b	
1b-16	Cr	127.8 (40.4)	SmC	240.4 (3.96)	SmA
		118.0 (41.0)		234.0 ^b	
1b-16	Cr	124.8 (52.2)	SmC	237.0 ^b	SmA
		116.2 (48.9)		231.0 ^b	
		228.0 ^b		234.0 ^b	
		215.0 ^b		237.5 (8.89)	
		213.0 ^b		234.2 (9.69)	
				231.6 (9.50)	
				218.1 (10.7)	
				216.4 (10.0)	

^a: *n* is the carbon number of alkoxy groups. Cr₁, Cr₂ = crystal, SmC = smectic C, SmA = smectic A, nematic = N, and I = isotropic phase. ^b: obtained by POM.

Compounds **1a-n** have lower melting and clearing temperatures than those of compounds **1b-n**. The clearing temperatures of **1a-n** decreased with the length of the side chains; i.e., T_{cl} =166.8 °C ($n=6$)>155.1 °C ($n=12$)>143.2 °C ($n=16$), which indicated that van der Waal force between the alkoxy chains might be controlling force in deducing the mesophase. The temperature range the mesophases, either nematic or smectic C phase of **1a-n** was surprisingly short; ranging from ΔT =1.3 to 6.9 °C during the cooling process. The three compounds **1a-n** with shorter lateral chains ($n=6, 8, 10$) formed nematic phases, in contrast, all other compounds **1a-n** ($n=12, 14, 16$) exhibited smectic C phases. The phase was characterized and identified as nematic and smectic C phases, first by POM observation. A typical Schlieren texture or broken focal-conics texture under the polarizing microscopy was observed when cooled from isotropic liquid, as shown in Fig. 1. The nematic phase was also consistent with an observation of homeotropic domain under POM. A relatively smaller enthalpy

(ΔH =0.95–3.65 kJ/mol) for the transition of N→I phase was obtained. The mesomorphic behavior observed by **1a-n** was slightly improved over the nonmesogenic 2,5-(dialkoxyphenyl)-1,3,4-oxadiazoles^{7a} **3a**. The reasons might be two folds. The use of two lateral 4-naphthyl groups not only enhanced the π – π interactions but also increases its l/d aspect ratio. Both structural alternations often can better induce the formation of respective mesophases.

In contrast, their homolog 1,3,4-thiadiazoles **1b-n** showed an apparently improved mesomorphic behavior. Compounds **1b-n** showed a more kinetically stable mesomorphic behavior than that of compounds **1a-n**. Compounds **1b-n** were also mesogenic and formed enantiotropic mesomorphic behavior over a wider temperature range. The clearing temperatures of **1b-n** decreased with the carbon length of alkoxy chains, i.e., T_{cl} =287.7 °C ($n=6$)>239.6 °C ($n=12$)>218.1 °C ($n=16$), which were all much higher than those of **1a-n** by T_{cl} =118.9 °C ($n=6$) to 74.9 °C ($n=16$). The temperature ranges of mesophases were much wider than those of

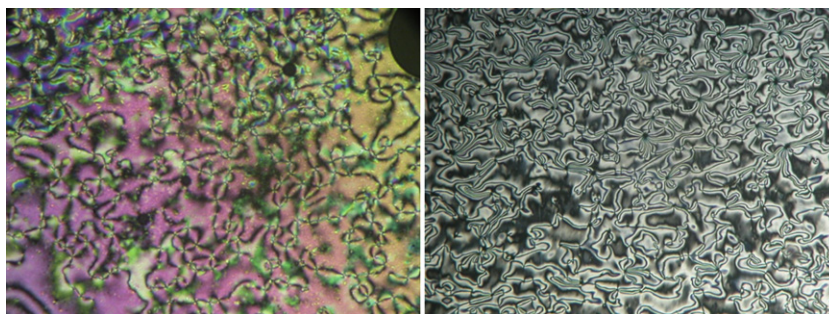


Fig. 1. Optical textures observed on the cooling process; N phase at 149 °C by **1a-10** (left) and SmC phase at 143.6 °C by **1a-14** (right).

compounds **1a-n**, and they decreased with the carbon length; i.e., $\Delta T_{\text{phase}}=147.3\text{ }^{\circ}\text{C}$ ($n=6$) $>112.0\text{ }^{\circ}\text{C}$ ($n=12$) $>91.3\text{ }^{\circ}\text{C}$ ($n=16$) during the cooling process. All transition temperatures in **1b-n** of smectic C \leftrightarrow smectic A phases both on heating and cooling processes were directly obtained by POM due to their smaller enthalpies not detected on DSC analysis. The three compounds **1b-n** with shorter lateral chains ($n=6, 8, 10$) formed nematic/smectic A/smectic C phases, whereas, all other compounds **1b-n** ($n=12, 14, 16$) exhibited smectic A/smectic C phases. The nematic, smectic A, and smectic C phases were identified by POM; a few typical textures shown in Fig. 2. The replacement of oxygen atom in **1a-n** by sulfur atom in **1b-n** much improved their liquid crystalline behavior. The larger sulfur atom incorporated was more polarized, leading to a larger dipole moment, which facilitated to the induction of mesophases. Also, a longer C–S bond distance and a smaller C–S–C angle of 1,3,4-thiadiazole unit favored the formation of a more rod-like molecular conformation. Such better linear conformation facilitated more efficient packing of molecules in the mesophases, compared to the bent-shaped 1,3,4-oxadiazoles. The thermal stability of compounds **1a-6** and **1b-6** was also characterized by thermogravimetric analyses (TGA), shown in Fig. 3. Two compounds showed excellent thermal stability above their clearing temperature. For example, the decomposition temperatures for a 5% weight loss for **1a-6** and **1b-6** were obtained at $T_d=398.5$ and $366.6\text{ }^{\circ}\text{C}$, respectively.

2.3. Variable-temperature powder XRD diffraction data

The powder X-ray diffraction experiment of compound **1b-6** was performed to confirm the structures of the smectic C and nematic phases. The X-ray diffraction plot was presented in Fig. 4. Due to the shorter temperature range of smectic A phases, the XRD diffraction was performed at 180 and 220 $^{\circ}\text{C}$. As indicated, it displayed a typical diffraction pattern with one strong peak at lower angle region, and a very weak and broad diffraction peak at wider angle. The strong diffraction peak at 180 $^{\circ}\text{C}$ with a d -spacing of 27.0 \AA was assigned as 001. This diffraction pattern was typically characteristic of a layer structure or the main periodicity of the system observed for SmC phases. Also, this d -spacing of 27.0 \AA was slightly smaller than

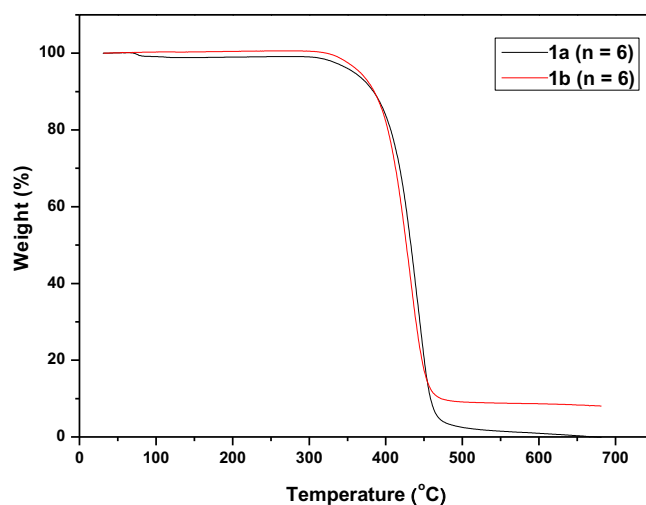


Fig. 3. TGA curves of compounds **1a-6** and **1b-6**.

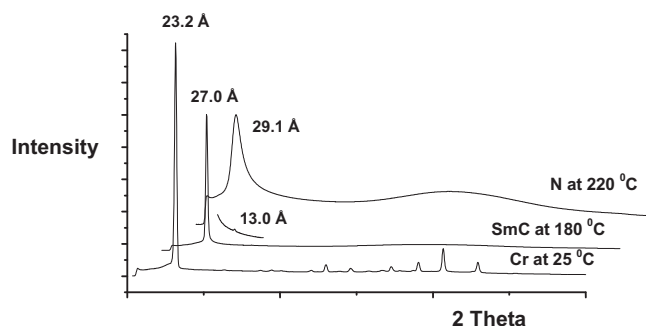


Fig. 4. The XRD diffraction plots of compound **1b-6** at 25.0, 180.0, and 220.0 $^{\circ}\text{C}$ during the cooling process.

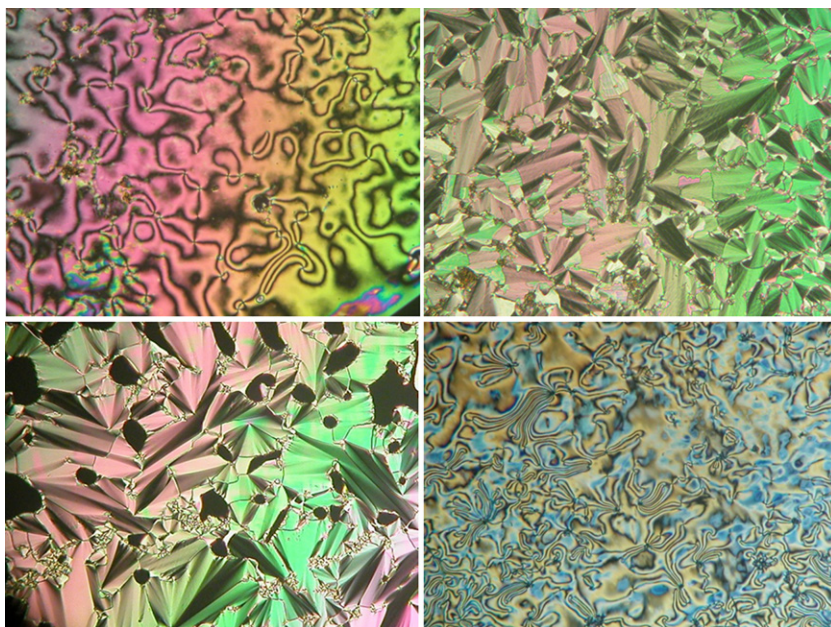


Fig. 2. Optical textures observed on the cooling process. Top plates: N phase at 244.0 $^{\circ}\text{C}$ (left) and SmC phase at 200.0 $^{\circ}\text{C}$ (right) by **1b-10**. Bottom plates: SmA phase at 236.0 $^{\circ}\text{C}$ (left) and SmC phase at 210.0 $^{\circ}\text{C}$ (right) by **1b-12**.

31.5 Å, which was obtained from calculated molecular length by MM2 model. This might indicate that the molecules were tilted and/or the alkoxy chains were also slightly interdigitated. A very broad and weak peak at ~ 4.60 Å was observed, and this peak was assigned to the molten alkoxy chains. Fig. 5 shows the molecular arrangements in crystal and smectic C phases.

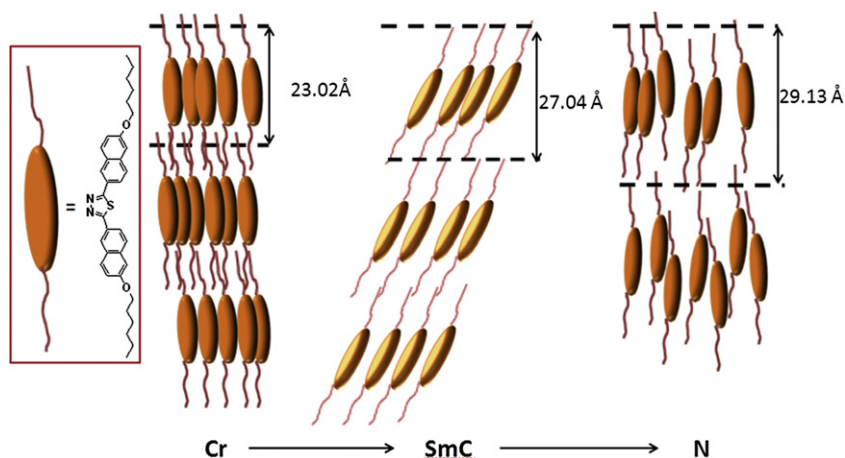


Fig. 5. Schematic illustration for molecular arrangements of Cr, smectic C and nematic phases in **1b-n**.

2.4. Optical properties

1,3,4-Oxadiazole derivatives were long known as potential light-emitting materials due to their photophysical and fluorescent properties. The luminescent properties observed by such compounds were often affected by the nature of substituents and/or conjugation length. The UV–vis absorption and the photoluminescence spectra of the two compounds **6a-6** and **6b-6** dissolved in THF were shown in Fig. 6. The absorption and emission

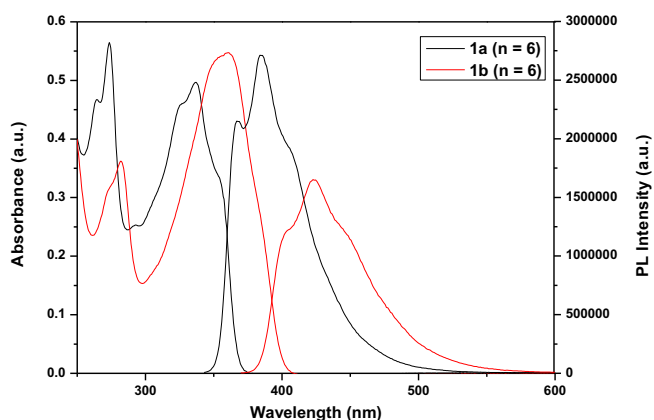


Fig. 6. Absorption and PL spectra of compounds **1a-6** and **1b-6** measured in THF at room temperature.

spectra were very similar in shape. The absorption spectra showed two peak absorbance wavelengths at ca. 273 and 337 nm for the 1,3,4-oxadiazoles **1a-6**. The two λ_{\max} peaks shifted to approximately 282 and 360 nm for 1,3,4-thiadiazole **1b-6**, summarized in Table 2. The first absorption λ_{\max} bands at 273 and 282 nm were attributed to the transitions in the lateral naphthalene rings of the molecule due to the high molar absorption coefficient. The second λ_{\max} bands at 337–360 nm were due to the heteroaromatic moieties. This increase of λ_{\max} from 273 to 282 nm was probably

Table 2
Summary of photophysical properties^a of compounds **1a-6** and **1b-6**

Compound	$\lambda_{\text{abs}}/\text{nm}$	$\lambda_{\text{em}}/\text{nm}$	Stokes shift/nm
1a-6	264; ^b 273; 337	367; ^b 385; 406 ^b	48
1b-6	274; ^b 282; 360	405; ^b 423; 448 ^b	63

^a Measured in THF solution at 25 °C.

^b Shoulder peak.

attributed to a lowering of $\pi-\pi^*$ band gap energy caused by electron-donating ability of sulfur atom into the aromatic moieties. These two wavelengths at $\lambda_{\max}=337$ and 360 nm were used to obtain the PL spectra. A similar trend was also observed in the photoluminescence spectra. The emission peaks were much broader, which occurred at ca. 385 and 423 nm measured in THF for **1a-6** and **1b-6**, respectively. The emitting color was ranged between blue and purple. The Stokes shifts to these two compounds are 48 nm (**1a-6**) and 63 nm (**1b-6**). The maximum at 385 and 423 nm can be attributed to the oxadiazoles and thiadiazole emitters while the maximum can be due to the naphthalene-containing chain segments. The carbon length of the alkoxy group has no influence on the fluorescence emitting spectrum of their solution states.

3. Conclusions

Two new series of 1,3,4-oxadiazoles **1a-n** and thiadiazoles **1b-n** were prepared, characterized, and their mesomorphic behavior investigated. Both series were all mesogenic, exhibiting N, SmA or/and SmC phases. 1,3,4-Thiadiazoles are kinetically more stable than 1,3,4-oxadiazoles. 1,3,4-Thiadiazoles have a wider temperature range of mesophases over that of 1,3,4-oxadiazoles, which were attributed to the more polarized sulfur atom incorporated. Two naphthyl rings 2,5-substituted to the central 1,3,4-oxadiazoles have better improved the mesomorphism, over their nonmesogenic homologs, 2,5-bis(alkoxyphenyl)-1,3,4-oxadiazoles **3a**. Both series of **1a-n** and **1b-n** have excellent thermal stabilities and also were excellent blue emitters. This work demonstrated that an improved mesophase with a much wider temperature range could be obtained by use of sulfur atom incorporated and naphthalene rings in 1,3,4-thiadiazoles.

4. Experimental section

4.1. General

¹H and ¹³C NMR spectra were measured on a Bruker DRX-300. DSC thermographs were carried out on a Mettler DSC 822. All

phase transitions are determined by a scan rate of 10.0 °C/min. Optical polarized microscopy was carried out on Zeiss Axioplan 2 equipped with a hot stage system of Mettler FP90/FP82HT. The UV–vis absorption and fluorescence spectra were obtained using SHIMADZU-UV-3150 spectrometer and HORIBA-JOBIN YVON spectrophotometer. Elemental analysis for carbon, hydrogen, and nitrogen was conducted at Instrumentation Center, National Taiwan University on a Heraeus CHN-O-Rapid elemental analyzer. The powder diffraction data were collected from the Wiggler-A beam line of the National Synchrotron Radiation Research Center with the wavelength of 1.3263 Å.

4.2. Syntheses of compounds 1a–n and 1b–n

4.2.1. 6-(Hexyloxy)-N'-(6-(hexyloxy)-2-naphthoyl)-2-naphthohydrazide. The solution of 6-(hexyloxy)-2-naphthoic acid (5.0 g, 0.0148 mol) was refluxed in 20 mL of thionyl chloride for 4 h under nitrogen atmosphere. The excess thionyl chloride was removed under reduced pressure. The paste was redissolved in dried 20 mL of THF, and to which hydrazine monohydrate (2.5 ml) was slowly added. Light yellow solids were precipitated, and the mixture was stirred for another 6 h at room temperature. The solids were then collected, and the products isolated as yellow solids were obtained after recrystallization twice from THF. Yield 87%. ¹H NMR (300 MHz, DMSO): δ 0.90 (br, –CH₃, 6H), 1.33–1.45 (m, –CH₂, 12H), 1.78–1.80 (m, –CH₂, 4H), 4.13 (t, OCH₂, 4H, *J*=6 Hz), 7.25 (d, Ar–H, 2H, *J*=8.7 Hz), 7.41 (br, Ar–H, 2H), 7.90–7.98 (m, Ar–H, 6H), 8.50 (br, Ar–H, 2H), 10.60 (br, –NH, 2H). ¹³C NMR (75 MHz, DMSO): δ 14.97, 23.13, 26.28, 29.62, 32.05, 68.76, 107.63, 120.78, 125.59, 127.90, 128.40, 128.57, 128.97, 131.60, 137.17, 159.22, 167.06.

4.2.2. 2,5-Bis(6-(dodecyloxy)naphthalen-2-yl)-1,3,4-oxadiazole (1a-12). The mixture of 6-(dodecyloxy)-N'-(6-(dodecyloxy)-2-naphthoyl)-2-naphthohydride (1.0 g, 1.41 mmol) and phosphoryl chloride was gently refluxed for 8 h under nitrogen atmosphere. Water was slowly added, and the solution was stirred with dilute aqueous NaOH (1.0 M) added for 4 h. The resulting yellow-green solids were collected. The products isolated as white solids were obtained after three times recrystallization from hot THF. Yield 72%. ¹H NMR (300 MHz, CDCl₃): δ 0.85 (t, –CH₃, 6H, *J*=6.3 Hz), 1.24–1.50 (m, –CH₂, 36H), 1.79–1.89 (m, –CH₂, 4H), 4.08 (t, –OCH₂, 4H, *J*=6.3 Hz), 7.14 (s, Ar–H, 2H), 7.15–7.22 (m, Ar–H, 2H), 7.84 (t, Ar–H, 4H, *J*=9.9 Hz), 8.16 (d, Ar–H, 2H, *J*=8.7 Hz), 8.55 (s, Ar–H, 2H). MS (FAB): calcd for M⁺: C₄₆H₆₂N₂O₃: 691.00. Found: 691.2. Anal. Calcd for C₄₆H₆₂N₂O₃: C, 79.96; H, 9.04. Found: C, 79.61; H, 9.01.

4.2.3. 2,5-Bis(6-(hexyloxy)naphthalen-2-yl)-1,3,4-oxadiazole (1a-6). White solid; yield 70%. ¹H NMR (CDCl₃): δ 0.92 (t, –CH₃, 6H, *J*=3.5 Hz), 1.34–1.39 (m, –CH₂, 12H), 1.82–1.89 (m, –CH₂, 4H), 4.08 (t, –OCH₂, 4H, *J*=6.6 Hz), 7.15 (s, Ar–H, 2H), 7.20–7.23 (m, Ar–H, 2H), 7.85 (t, Ar–H, 4H, *J*=9.9 Hz), 8.17 (d, Ar–H, 2H, *J*=8.4 Hz), 8.55 (s, Ar–H, 2H). MS (FAB): calcd for M⁺: C₃₄H₃₈N₂O₃: 522.68. Found: 522.9. Anal. Calcd for C₃₄H₃₈N₂O₃: C, 78.13; H, 7.33. Found: C, 78.47; H, 7.42.

4.2.4. 2,5-Bis(6-(octyloxy)naphthalen-2-yl)-1,3,4-oxadiazole (1a-8). White solid; yield 71%. MS (FAB): calcd for M⁺: C₃₈H₄₆N₂O₃: 578.78. Found: 579.1. Anal. Calcd for C₃₈H₄₆N₂O₃: C, 78.86; H, 8.01. Found: C, 78.92; H, 8.12.

4.2.5. 2,5-Bis(6-(decyloxy)naphthalen-2-yl)-1,3,4-oxadiazole (1a-10). White solid; yield 70%. ¹H NMR (300 MHz, CDCl₃): δ 0.86 (t, –CH₃, 6H, *J*=6.3 Hz), 1.25–1.46 (m, –CH₂, 28H), 1.79–1.88 (m, –CH₂, 4H), 4.07 (t, –OCH₂, 4H, *J*=6.6 Hz), 7.15 (s, Ar–H, 2H), 7.19–7.22 (m, Ar–H, 2H), 7.83 (t, Ar–H, 4H, *J*=9.9 Hz), 8.16 (d, Ar–H, 2H, *J*=7.2 Hz), 8.53 (s, Ar–H, 2H). ¹³C NMR (75 MHz, CDCl₃): δ 14.10, 22.67, 26.08, 29.16, 29.32, 29.40, 29.57, 31.89, 68.21, 106.65, 118.76, 120.32,

123.81, 127.10, 127.66, 128.17, 130.30, 136.34, 158.87, 164.76. MS (FAB): calcd for M⁺: C₄₂H₅₄N₂O₃: 634.89. Found: 635.2. Anal. Calcd for C₄₂H₅₄N₂O₃: C, 79.45; H, 8.57. Found: C, 79.19; H, 8.58.

4.2.6. 2,5-Bis(6-(tetradecyloxy)naphthalen-2-yl)-1,3,4-oxadiazole (1a-14). White solid; yield 73%. ¹H NMR (300 MHz, CDCl₃): δ 0.85 (t, –CH₃, 6H, *J*=6 Hz), 1.24–1.39 (m, –CH₂, 44H), 1.83–1.87 (m, –CH₂, 4H), 4.09 (t, –OCH₂, 4H, *J*=6.3 Hz), 7.16 (s, Ar–H, 2H), 7.20–7.21 (m, Ar–H, 2H), 7.85 (t, Ar–H, 4H, *J*=9.6 Hz), 8.18 (d, Ar–H, 2H, *J*=6.9 Hz), 8.56 (s, Ar–H, 2H). MS (FAB): calcd for M⁺: C₅₀H₇₀N₂O₃: 747.10. Found: 747.5. Anal. Calcd for C₅₀H₇₀N₂O₃: C, 80.38; H, 9.44. Found: C, 80.40; H, 9.41.

4.2.7. 2,5-Bis(6-(hexadecyloxy)naphthalen-2-yl)-1,3,4-oxadiazole (1a-16). White solid; yield 72%. MS (FAB): calcd for M⁺: C₅₄H₇₈N₂O₃: 803.21. Found: 803.4. Anal. Calcd for C₅₄H₇₈N₂O₃: C, 80.75; H, 9.79. Found: C, 80.87; H, 9.86.

4.2.8. 2,5-Bis(6-(dodecyloxy)naphthalen-2-yl)-1,3,4-thiadiazole (1b-12). Under nitrogen atmosphere. The solution of 6-(dodecyloxy)-N'-(6-(dodecyloxy)-2-naphthoyl)-2-naphthohydrazide (1.0 g, 1.41 mmol) dissolved in 20 mL of pyridine was added phosphorus(V) sulfide (2.19 g, 9.87 mmol). The solution was refluxed for 24 h. The solution was then extracted twice with CH₂Cl₂/H₂O, and organic layers were dried over anhydrous MgSO₄ and concentrated to give yellow solids. The products isolated as light yellow solids were obtained by recrystallization from CH₂Cl₂/CH₃OH. Yield 70%. ¹H NMR (300 MHz, CDCl₃): δ 0.86 (t, –CH₃, 6H, *J*=6 Hz), 1.25–1.51 (m, –CH₂, 36H), 1.82–1.87 (m, –CH₂, 4H), 4.08 (t, –OCH₂, 4H, *J*=6.3 Hz), 7.15 (s, Ar–H, 2H), 7.20 (d, Ar–H, 2H, *J*=9 Hz), 7.79–7.84 (m, Ar–H, 4H), 8.10 (d, Ar–H, 2H, *J*=8.7 Hz), 8.37 (s, Ar–H, 2H). ¹³C NMR (75 MHz, CDCl₃): δ 13.92, 22.49, 25.89, 28.98, 29.15, 29.21, 29.41, 68.01, 106.43, 120.09, 124.84, 127.51, 130.02, 135.96, 158.49, 167.96. MS (FAB): calcd for M⁺: C₄₆H₆₂N₂O₂S: 707.06. Found: 707.3. Anal. Calcd for C₄₆H₆₂N₂O₂S: C, 78.14; H, 8.84. Found: C, 78.01; H, 8.30.

4.2.9. 2,5-Bis(6-(hexyloxy)naphthalen-2-yl)-1,3,4-thiadiazole (1b-6). Light yellow solid; yield 72%. ¹H NMR (300 MHz, CDCl₃): δ 0.91 (t, –CH₃, 6H, *J*=7.2 Hz), 1.33–1.50 (m, –CH₂, 12H), 1.76–1.86 (m, –CH₂, 4H), 4.02 (t, –OCH₂, 4H, *J*=6.6 Hz), 7.07 (s, Ar–H, 2H), 7.16 (dd, Ar–H, 2H, *J*₁=6.6 Hz, *J*₂=2.4 Hz), 7.72–7.79 (m, Ar–H, 4H), 8.03 (dd, Ar–H, 2H, *J*₁=6.9 Hz, *J*₂=1.8 Hz), 8.28 (s, Ar–H, 2H). ¹³C NMR (75 MHz, CDCl₃): δ 14.03, 22.59, 25.74, 29.13, 31.59, 68.12, 106.52, 120.14, 124.95, 125.30, 127.57, 127.82, 128.36, 130.11, 135.99, 158.52, 167.99. MS (FAB): calcd for M⁺: C₃₄H₃₈N₂O₂S: 538.74. Found: 539.1. Anal. Calcd for C₃₄H₃₈N₂O₂S: C, 75.80; H, 7.11. Found: C, 77.77; H, 7.10.

4.2.10. 2,5-Bis(6-(octyloxy)naphthalen-2-yl)-1,3,4-thiadiazole (1b-8). Light yellow solid; yield 71%. MS (FAB): M⁺: calcd for C₃₈H₄₆N₂O₂S: 594.85. Found: 595.2. Anal. Calcd for C₃₈H₄₆N₂O₂S: C, 76.73; H, 7.79. Found: C, 76.88; H, 7.90.

4.2.11. 2,5-Bis(6-(decyloxy)naphthalen-2-yl)-1,3,4-thiadiazole (1b-10). Light yellow solid; yield 74%. ¹H NMR (300 MHz, CDCl₃): δ 0.87 (t, –CH₃, 6H, *J*=6.6 Hz), 1.27–1.51 (m, –CH₂, 20H), 1.79–1.88 (m, –CH₂, 4H), 4.07 (t, –OCH₂, 4H, *J*=6.6 Hz), 7.13 (s, Ar–H, 2H), 7.19 (dd, Ar–H, 2H, *J*₁=6.6 Hz, *J*₂=2.1 Hz), 7.79 (t, Ar–H, 4H, *J*=8.7 Hz), 8.08 (dd, Ar–H, 2H, *J*₁=6.9 Hz, *J*₂=1.5 Hz), 8.34 (s, Ar–H, 2H). ¹³C NMR (75 MHz, CDCl₃): δ 14.10, 22.67, 26.08, 29.18, 29.32, 29.41, 31.89, 68.18, 106.61, 120.22, 125.01, 125.32, 127.64, 127.94, 128.41, 130.16, 136.07, 158.60, 168.08. MS (FAB): calcd for M⁺: C₄₂H₅₄N₂O₂S: 650.96. Found: 651.5. Anal. Calcd for C₄₂H₅₄N₂O₂S: C, 77.49; H, 8.36. Found: C, 77.94; H, 8.38.

4.2.12. 2,5-Bis(6-(tetradecyloxy)naphthalen-2-yl)-1,3,4-thiadiazole (1b-14). Light yellow solid; yield 73%. ¹H NMR (300 MHz, CDCl₃):

δ 0.86 (t, $-\text{CH}_3$, 6H, $J=6.3$ Hz), 1.24–1.49 (m, $-\text{CH}_2$, 44H), 1.82–1.86 (m, $-\text{CH}_2$, 4H), 4.08 (t, $-\text{OCH}_2$, 4H, $J=6.6$ Hz), 7.13 (s, Ar–H, 2H), 7.19 (d, Ar–H, 2H, $J=8.7$ Hz), 7.80 (t, Ar–H, 4H, $J=8.1$ Hz), 8.09 (d, Ar–H, 2H, $J=8.4$ Hz), 8.36 (s, Ar–H, 2H). ^{13}C NMR (75 MHz, CDCl_3): δ 14.12, 22.69, 26.10, 29.19, 29.67, 31.93, 68.21, 106.64, 120.27, 125.04, 125.26, 127.69, 128.03, 128.44, 130.19, 136.13, 158.67, 168.14. MS (FAB): calcd for M^+ : $\text{C}_{50}\text{H}_{70}\text{N}_2\text{O}_2\text{S}$: 763.17. Found: 763.6. Anal. Calcd for $\text{C}_{50}\text{H}_{70}\text{N}_2\text{O}_2\text{S}$: C, 78.69; H, 9.25. Found: C, 78.71; H, 9.26.

4.2.13. 2,5-Bis(6-(hexadecyloxy)naphthalen-2-yl)-1,3,4-thiadiazole (**1b-16**). Light yellow solid; yield 72%. ^1H NMR (300 MHz, CDCl_3): δ 0.84 (t, $-\text{CH}_3$, 6H, $J=6.3$ Hz), 1.24–1.48 (m, $-\text{CH}_2$, 52H), 1.83–1.84 (m, $-\text{CH}_2$, 4H), 4.07 (t, $-\text{OCH}_2$, 4H, $J=6.6$ Hz), 7.14 (s, Ar–H, 2H), 7.20 (d, Ar–H, 2H, $J=8.7$ Hz), 7.84 (t, Ar–H, 4H, $J=8.4$ Hz), 8.09–8.19 (m, Ar–H, 2H), 8.38 (s, Ar–H, 2H). ^{13}C NMR (75 MHz, CDCl_3): δ 14.11, 22.69, 26.10, 29.37, 29.68, 31.92, 68.24, 106.66, 120.35, 125.04, 125.26, 127.78, 128.23, 128.39, 130.26, 136.13, 158.66, 163.20. MS (FAB): calcd for M^+ : $\text{C}_{54}\text{H}_{78}\text{N}_2\text{O}_2\text{S}$: 650.96. Found: 651.3. Anal. Calcd for $\text{C}_{54}\text{H}_{78}\text{N}_2\text{O}_2\text{S}$: C, 79.16; H, 9.60. Found: C, 79.06; H, 9.64.

Acknowledgements

We thank the National Science Council of Taiwan, ROC for funding (NSC 100-2113-M-008-002-MY2) in generous support of this work.

Supplementary data

The synthetic procedures of some compounds and DSC thermographs. Supplementary data associated with this article can be found in the online version, at <http://dx.doi.org/10.1016/j.tet.2012.06.092>.

References and notes

- (a) Zheng, Y.; Batsanov, A. S.; Bryce, M. R. *Inorg. Chem.* **2011**, *50*, 3354–3362; (b) Bolton, O.; Kim, J. J. *Mater. Chem.* **2007**, *17*, 1981–1988; (c) Seed, A. *Chem. Soc. Rev.* **2007**, *36*, 2046–2069; (d) Kang, S.; Saito, Y.; Watanabe, N.; Tokita, M.; Takanishi, Y.; Takezoe, H.; Watanabe, J. *J. Phys. Chem. B* **2006**, *110*, 5205–5214; (e) Han, J.; Chui, S. S. Y.; Che, C. M. *Chem. Asian J.* **2006**, *1*, 814–825; (f) Kamtekar, K. T.; Wang, C.; Bettington, S.; Batsanov, A. S.; Perepichka, I. F.; Bryce, M. R.; Ahn, J. H.; Rabinal, M.; Petty, M. C. *J. Mater. Chem.* **2006**, *16*, 3823–3835; (g) Ichikawa, M.; Kawaguchi, T.; Kobayashi, K.; Miki, T.; Furukawa, K.; Koyama, T.; Taniguchi, Y. *J. Mater. Chem.* **2006**, *16*, 221–225; (h) Shao, P.; Huang, B.; Chen, L.; Liu, Z.; Qin, J.; Gong, H.; Ding, S.; Wang, Q. *J. Mater. Chem.* **2005**, *15*, 4502–4506; (i) Cristiano, R.; De, O.; Santos, D. M. P.; Gallardo, H. *Liq. Cryst.* **2005**, *32*, 7–14; (j) Oyston, S.; Wang, C.; Perepichka, I. F.; Batsanov, A. S.; Bryce, M. R.; Ahn, J. H.; Petty, M. C. *J. Mater. Chem.* **2005**, *15*, 5164–5173; (k) Hughes, G.; Bryce, M. R. *J. Mater. Chem.* **2005**, *15*, 94–107; (l) Madsen, L. A.; Dingemans, T. J.; Nakata, M.; Samulski, E. T. *Phys. Rev. Lett.* **2004**, *92*, 145505/1–145505/4; (m) Hughes, G.; Kreher, D.; Wang, C.; Batsanov, A. S.; Bryce, M. R. *Org. Biomol. Chem.* **2004**, *2*, 3363–3367; (n) Wang, C.; Batsanov, A. S.; Bryce, M. R. *Chem. Commun.* **2004**, 578–579.
- Dimitrowa, K.; Hauschild, J.; Zschke, H.; Schubert, H. *J. Prakt. Chem.* **1980**, *322*, 933–944.
- (a) Qu, S.; Wang, L.; Liu, X.; Li, M. *Chem.—Eur. J.* **2011**, *17*, 3512–3518; (b) Barberá, J.; Godoy, M. A.; Hidalgo, P. I.; Parra, M. L.; Ullo, J. A.; Vergara, J. M. *Liq. Cryst.* **2011**, *38*, 679–688; (c) Zhang, P.; Bai, B.; Wang, H.; Qu, S.; Yu, Z.; Ran, X.; Li, M. *Liq. Cryst.* **2009**, *36*, 7–12; (d) Srivastava, R. M.; Ricardo, A. W.; Filho, N.; Schneider, R.; Vieira, A.; Gallardo, H. *Liq. Cryst.* **2008**, *35*, 737–742; (e) Wang, H.; Zhang, F.; Bai, B.; Zhang, P.; Shi, J.; Yu, D.; Zhao, Y.; Wang, Y.; Li, M. *Liq. Cryst.* **2008**, *35*, 905–912; (f) Zhang, P.; Qu, S.; Wang, H.; Bai, B.; Li, M. *Liq. Cryst.* **2008**, *35*, 389–394; (g) Chai, C.; Yang, Q.; Fan, X.; Chen, X.; Shen, Z.; Zhou, Q. *Liq. Cryst.* **2008**, *35*, 133–141; (h) Qu, S.; Li, M. *Tetrahedron* **2007**, *63*, 12429–12436.
- (a) Tang, J.; Huang, R.; Gao, H.; Cheng, X.; Prehm, M.; Tschierske, C. *RSC Adv.* **2012**, *2*, 2842–2847; (b) Vieira, A. A.; Gallardo, H.; Barbera, J.; Romero, P.; Serrano, J. L.; Sierra, T. *J. Mater. Chem.* **2011**, *21*, 5916–5922; (c) Gallardo, H.; Ferreira, M.; Vieira, A. A.; Westphal, E.; Molin, F.; Eccher, J.; Bechtold, I. H. *Tetrahedron* **2011**, *67*, 9491–9499; (d) Yelamaggad, C. V.; Achalkumar, A. D.; Rao, D. S. R.; Prasad, S. K. *J. Org. Chem.* **2009**, *74*, 3168–3171.
- (a) Tschierske, C.; Photinos, D. J. *J. Mater. Chem.* **2010**, *21*, 4263–4294; (b) Zafiroopoulos, Z. A.; Lin, W.; Samulski, E. T.; Dingemans, T. J.; Picken, S. J. *Liq. Cryst.* **2009**, *36*, 649–656; (c) Dingemans, T. J.; Madsen, L. A.; Zafiroopoulos, N. A.; Lin, W.; Samulski, E. T. *Phil. Trans. R. Soc. A* **2006**, *364*, 2681–2696.
- (a) Picken, S. J.; Dingemans, T. J.; Madsen, L. A.; Francescangeli, O.; Samulski, E. T. *Liq. Cryst.* **2012**, *39*, 19–23; (b) Prajapati, A. K.; Modi, V. *Liq. Cryst.* **2011**, *38*, 191–199; (c) Bates, M. A. *Chem. Phys. Lett.* **2007**, *437*, 189–192; (d) Acharya, B. R.; Primak, A.; Dingemans, T. J.; Samulski, E. T.; Kumar, S. *Pramana-J. Phys.* **2003**, *61*, 231–237; (e) Dingemans, T. J.; Murthy, N. S.; Samulski, E. T. *J. Phys. Chem. B* **2001**, *105*, 8845–8860.
- (a) Wang, H.; Zheng, Z.; Shen, D. *Liq. Cryst.* **2012**, *39*, 99–103; (b) Wang, L.; Yu, L.; Xiao, X.; Wang, Z.; Yang, P.; He, W.; Yang, H. *Liq. Cryst.* **2012**, *39*, 629–638; (c) Lai, C. K.; Ke, Y. C.; Su, J. C.; Shen, C.; Li, W. R. *Liq. Cryst.* **2002**, *29*, 915–920; (d) Wen, C. R.; Wang, Y. J.; Wang, H. C.; Sheu, H. S.; Lee, G. H.; Lai, C. K. *Chem. Mater.* **2005**, *17*, 1646–1654.
- Dingemans, T. J.; Samulski, E. T. *Liq. Cryst.* **2000**, *27*, 131–136.
- Prajapati, A. K.; Modi, V. *Liq. Cryst.* **2010**, *37*, 407–415.
- (a) Han, J.; Zhang, M.; Wang, F.; Geng, Q. *Liq. Cryst.* **2010**, *37*, 1471–1478; (b) Parra, M. L.; Elgueta, E. Y.; Jimenez, V.; Hidalgo, P. I. *Liq. Cryst.* **2009**, *36*, 301–317; (c) Han, J.; Zhang, F. Y.; Wang, J. Y.; Wang, Y. M.; Pang, M. L.; Meng, J. B. *Liq. Cryst.* **2009**, *36*, 825–833.
- Han, J.; Zhang, F. Y.; Chen, Z.; Wang, J. Y.; Zhu, L. R.; Pang, M. L.; Meng, J. B. *Liq. Cryst.* **2008**, *35*, 1359–1365.
- (a) Prajapati, A. K.; Modi, V. *Phase Transitions* **2010**, *83*, 634–649; (b) Tomma, J. H.; Rouil, I. H.; Al-Dujaili, A. H. *Mol. Cryst. Liq. Cryst.* **2009**, *501*, 3–19; (c) Han, J.; Chang, X. Y.; Wang, Y. M.; Pang, M. L.; Meng, J. B. *J. Mol. Struct.* **2009**, *937*, 122–130; (d) Han, J.; Chang, X. Y.; Zhu, L. R.; Wang, Y. M.; Meng, J. B.; Lai, S. W.; Chui, S. S. Y. *Liq. Cryst.* **2008**, *35*, 1379–1394; (e) He, C. F.; Richards, G. J.; Kelly, S. M.; Contoret, A. E. A.; O'Neill, M. *Liq. Cryst.* **2007**, *34*, 1249–1267; (f) Liao, C. T.; Wang, Y. J.; Huang, C. S.; Sheu, H. S.; Lee, G. H.; Lai, C. K. *Tetrahedron* **2007**, *63*, 12427–12445.
- Lehmann, M.; Seltmann, J.; Auer, A. A.; Prochnow, E.; Benedikt, U. *J. Mater. Chem.* **2009**, *19*, 1978–1988.